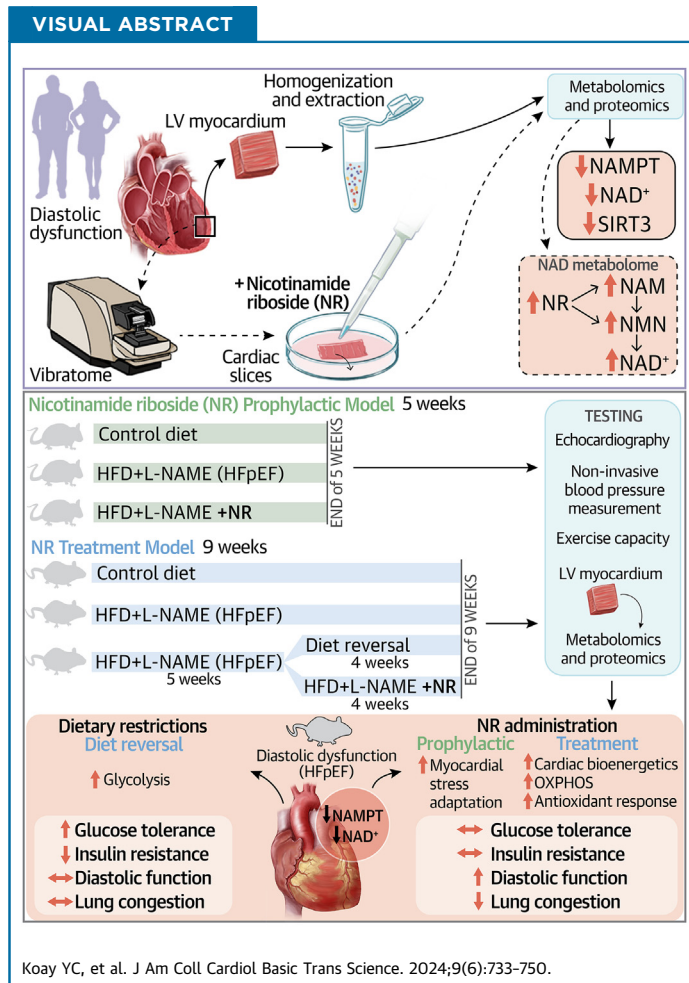


ORIGINAL RESEARCH - CLINICAL

# The Efficacy of Risk Factor Modification Compared to NAD<sup>+</sup> Repletion in Diastolic Heart Failure



Yen Chin Koay, PhD,<sup>a,b,c</sup> Ren Ping Liu, BS,<sup>a,b,c</sup> Bailey McIntosh, BS,<sup>a,b,c</sup> Niv Vigder, BS,<sup>b,c,d</sup> Serlin Lauren, BS,<sup>a,b,c</sup> Angela Yu Bai, BS,<sup>a,c,d</sup> Saki Tomita, BS,<sup>a,c</sup> Desmond Li, PhD,<sup>e</sup> Dylan Harney, PhD,<sup>c,d</sup> Benjamin Hunter, PhD,<sup>b,c,f</sup> Yunwei Zhang, PhD,<sup>c,g</sup> Jean Yang, PhD,<sup>c,g</sup> Paul Bannon, MD, PhD,<sup>a,b,c,h,i</sup> Ashleigh Philp, PhD,<sup>j,k</sup> Andrew Philp, PhD,<sup>c,l,m</sup> David M. Kaye, MD, PhD,<sup>n,o,p</sup> Mark Larance, PhD,<sup>b,c</sup> Sean Lal, MD, PhD,<sup>a,b,c,f,q,\*</sup> John F. O'Sullivan, MD, PhD<sup>a,b,c,q,r,\*</sup>



**HIGHLIGHTS**

- The feasibility of NAD<sup>+</sup> repletion in human myocardial tissue using the NAD precursor NR is demonstrated in our study.
- In a preclinical model, it is demonstrated that both prophylactic and therapeutic NAD<sup>+</sup> repletion is equally effective in addressing HFpEF.
- Despite favorable effects on cardiac metabolism, the HFpEF phenotype is not rescued by dietary intervention and weight loss. In contrast, the findings in our preclinical study suggest that NAD<sup>+</sup> repletion emerges as a promising strategy for phenotype rescue.

From the <sup>a</sup>Cardiometabolic Medicine Group, The University of Sydney, Sydney, New South Wales, Australia; <sup>b</sup>School of Medical Sciences, Faculty of Medicine and Health, The University of Sydney, Sydney, New South Wales, Australia; <sup>c</sup>Charles Perkins Centre, The University of Sydney, Sydney, New South Wales, Australia; <sup>d</sup>School of Life and Environmental Sciences, Faculty of Science, The University of Sydney, Sydney, New South Wales, Australia; <sup>e</sup>BCAL Diagnostics, National Innovation Centre, Eveleigh, New South Wales, Australia; <sup>f</sup>Precision Cardiovascular Laboratory, The University of Sydney, New South Wales, Australia; <sup>g</sup>School of

## ABBREVIATIONS AND ACRONYMS

**AMD** = age-matched donor  
**ATP** = adenosine triphosphate  
**CoA** = coenzyme A  
**DCM** = delayed cardiomyopathy  
**E/A** = early to late diastolic transmitral flow velocity  
**GLS** = global longitudinal strain  
**GSH** = glutathione  
**HCM** = hypertrophic cardiomyopathy  
**HF** = heart failure  
**HFD** = high-fat diet  
**HFpEF** = heart failure with preserved ejection fraction  
**HOcm** = hypertrophic obstructive cardiomyopathy  
**HOMA-IR** = homeostatic model assessment of insulin resistance  
**ICM** = ischemic cardiomyopathy  
**LV** = left ventricular  
**LVEF** = left ventricular ejection fraction  
**NAD<sup>+</sup>** = oxidized nicotinamide adenine dinucleotide  
**NADH** = reduced form of nicotinamide adenine dinucleotide  
**NADP<sup>+</sup>** = oxidized form of nicotinamide adenine dinucleotide phosphate  
**NADPH** = reduced form of nicotinamide adenine dinucleotide phosphate  
**NAMPT** = nicotinamide phosphoribosyltransferase  
**NR** = nicotinamide riboside  
**ROS** = reactive oxygen species  
**SIRT3** = sirtuin 3  
**TCA** = tricarboxylic acid

## SUMMARY

Heart failure (HF) with left ventricular diastolic dysfunction is a growing global concern. This study evaluated myocardial oxidized nicotinamide adenine dinucleotide (NAD<sup>+</sup>) levels in human systolic and diastolic HF and in a murine model of HF with preserved ejection fraction, exploring NAD<sup>+</sup> repletion as therapy. We quantified myocardial NAD<sup>+</sup> and nicotinamide phosphoribosyltransferase levels, assessing restoration with nicotinamide riboside (NR). Findings show significant NAD<sup>+</sup> and nicotinamide phosphoribosyltransferase depletion in human diastolic HF myocardium, but NR successfully restored NAD<sup>+</sup> levels. In murine HF with preserved ejection fraction, NR as preventive and therapeutic intervention improved metabolic and antioxidant profiles. This study underscores NAD<sup>+</sup> repletion's potential in diastolic HF management. (J Am Coll Cardiol Basic Trans Science 2024;9:733-750) © 2024 The Authors. Published by Elsevier on behalf of the American College of Cardiology Foundation. This is an open access article under the CC BY-NC-ND license (<http://creativecommons.org/licenses/by-nc-nd/4.0/>).

**H**eat failure with preserved ejection fraction (HFpEF) pathophysiology is driven by coexisting risk factors such as overweight/obesity, insulin resistance/type 2 diabetes mellitus, and hypertension.<sup>1,2</sup> These risk factors appear to be causal, and recent preclinical work suggests that both metabolic and hypertensive stressors are required for the development of HFpEF.<sup>3</sup> In older, obese HFpEF patients, intervention with caloric restriction and exercise (that leads to weight loss) can reduce left ventricular (LV) wall thickness and improve peak oxygen consumption (V<sub>O<sub>2</sub>max</sub>).<sup>4</sup> However, whether dietary intervention can rescue the full spectrum of established HFpEF remains unclear.

Together with the kidneys, the heart has the joint highest energy requirements and resting metabolic rate per unit mass (440 kcal/kg/d).<sup>5</sup> Unsurprisingly, the heart is abundant in mitochondria and has the greatest concentration of mitochondrial oxidized

nicotinamide adenine dinucleotide (NAD<sup>+</sup>) of all organs.<sup>6</sup> Recent preclinical work demonstrated that replenishment of myocardial NAD<sup>+</sup> can rescue HFpEF;<sup>7,8</sup> however, whether development of HFpEF can be prevented by pre-emptive supplementation with NAD<sup>+</sup> precursors has not been established. The specificity of NAD<sup>+</sup> depletion in diastolic vs systolic heart failure (HF) is unknown; furthermore, there are concerns about the biological feasibility of replenishing cardiac NAD<sup>+</sup> in human HF with lower protein levels of myocardial nicotinamide phosphoribosyltransferase (NAMPT).<sup>8</sup> Because stage A “at-risk” HF in HFpEF is easily identifiable by the presence of obesity, hypertension, insulin resistance/type 2 diabetes,<sup>9</sup> we sought to compare NAD<sup>+</sup> repletion prophylactically (stage A) vs therapeutically in established HF (stage C). With the increasing early recognition of risk factors in early HF as highlighted in the American College of Cardiology/American Heart Association/Heart Failure Society of America guidelines,<sup>9</sup> we also sought to examine the therapeutic potential of targeting HFpEF risk factors with dietary intervention and weight loss in comparison to the NAD<sup>+</sup> repletion strategies.

Mathematics and Statistics, Faculty of Science, The University of Sydney, Sydney, New South Wales, Australia; <sup>h</sup>Central Clinical School, Sydney Medical School, Faculty of Medicine and Health, The University of Sydney, Sydney, New South Wales, Australia; <sup>i</sup>Department of Cardiothoracic Surgery, Royal Prince Alfred Hospital, Camperdown, New South Wales, Australia; <sup>j</sup>School of Clinical Medicine, UNSW Medicine and Health, St Vincent's Healthcare clinical campus, UNSW, Sydney, New South Wales, Australia; <sup>k</sup>Centre for Inflammation, Centenary Institute and University of Technology Sydney, Faculty of Science, School of Life Sciences, Sydney, NSW, Australia; <sup>l</sup>Centre for Healthy Aging, Centenary Institute, Sydney, New South Wales, Australia; <sup>m</sup>School of Sport, Exercise and Rehabilitation Sciences, University of Technology Sydney, Ultimo, New South Wales, Australia; <sup>n</sup>Department of Cardiology, Alfred Hospital, Melbourne, Australia; <sup>o</sup>Heart Failure Research Group, Baker Heart and Diabetes Institute, Melbourne, Australia; <sup>p</sup>Faculty of Medicine, Monash University, Melbourne, Australia; <sup>q</sup>Department of Cardiology, Royal Prince Alfred Hospital, Camperdown, New South Wales, Australia; and the <sup>r</sup>Faculty of Medicine, Technische Universität Dresden, Dresden, Germany. \*Drs Lal and O'Sullivan contributed equally to this work.

The authors attest they are in compliance with human studies committees and animal welfare regulations of the authors' institutions and Food and Drug Administration guidelines, including patient consent where appropriate. For more information, visit the [Author Center](#).

Manuscript received November 16, 2023; revised manuscript received January 19, 2024, accepted January 19, 2024.

Therefore, we aimed to do the following: 1) compare levels of NAD<sup>+</sup> and NAMPT in human LV myocardium in diastolic and systolic HF; 2) determine the feasibility of replenishing human cardiac NAD<sup>+</sup>, where both NAD<sup>+</sup> and NAMPT are lower; and 3) using a murine model, compare the relative benefits and underlying mechanisms of dietary intervention, prophylactic nicotinamide riboside (NR) supplementation, and NR treatment following establishment of the HFpEF phenotype. By addressing these objectives, we aimed to further delineate the comparative role and the relative therapeutic potential of risk factor modification vs NAD<sup>+</sup> repletion in diastolic HF.

## METHODS

**ACQUISITION OF HUMAN MYOCARDIUM.** Human hypertrophic cardiomyopathy (HCM) and non-diseased LV myocardial samples from the anterior wall were procured as per the established ethical and governance guidelines of the Sydney Heart Bank.<sup>10-19</sup> Pathologic HCM myocardium was acquired from consenting patients with end-stage HF (NYHA functional classes III-IV) undergoing heart transplantation. Nonpathologic myocardium was acquired from nondiseased donor hearts that, at the time, were not able to be viably used for heart transplantation, often because of patient incompatibility or logistical challenges (not postmortem samples and histologically normal as per formal anatomic pathologic examination).<sup>10-19</sup>

Human hypertrophic obstructive cardiomyopathy (HOCM) LV myocardial samples from the muscular septum were acquired from patients undergoing a septal myectomy procedure (procured for the Sydney Heart Bank). Myocardium occluding the LV outflow tract was resected via access through the aortic valve. These patients showed normal systolic function but presented with diastolic dysfunction. Coordination and collaboration with local cardiothoracic surgeons at the time of surgery enabled the collection of all tissue within 40 minutes after aortic cross-clamp (HCM and donor) or resection (HOCM), ensuring that the tissue was not postmortem. This was later validated by histologic and RNA analyses.<sup>11,20</sup> Myocardium was delivered cardiopleged and on wet ice and used immediately in NR incubations or snap-frozen immediately in liquid nitrogen (-196 °C) and stored at -192 °C until use.

These harvesting and storage methods are approved by the Human Research Ethics Committee at The University of Sydney (USYD 2021/122). [Supplemental Table 1](#) shows the characteristics of nondiseased control individuals, patients with

systolic (delayed cardiomyopathy [DCM] and ischemic cardiomyopathy [ICM]) and diastolic (HOCM and HCM) impairments. The detailed methodology for NR incubation in heart slices can be found in the [Supplemental Appendix](#).

**ANIMAL EXPERIMENTS.** All procedures involving animals received prior ethics approval from the Institutional Animal Ethics Committee at the University of Sydney (ethics number 2017/1294). Male and female C57BL/6J mice were obtained from Animal Bioresources (Moss Vale). They were first acclimatized for 2 weeks on normal chow. Mice were maintained on a 12-hour light-dark cycle.

For the 5-week study, mice aged 10 to 12 weeks were randomly assigned to control and HFpEF (subjected to high-fat diet [HFD] + 0.5 g/L of N<sup>[w]</sup>-nitro-L-arginine methyl ester [L-NAME] treatment) (n = 6-17/group). For the 9-week study, 3-month-old male mice and 4-month-old female mice were divided into 4 groups and randomly assigned to control, HFpEF (administered HFD + L-NAME), recovery (removal of HFD + L-NAME at 5 weeks and replacement with chow and normal drinking water), and NAD<sup>+</sup> precursor NR of ~500 mg/kg daily (commencement of treatment at 5 weeks with simultaneous administration of HFD + L-NAME for a further 4 weeks) groups (n = 8 or 9 per group). For the prophylactic NR group, mice were fed HFD incorporated with NR and drinking water containing L-NAME (since the initiation of disease, similar to that of HFpEF mice) until study termination. Details can be found in the [Supplemental Appendix](#).

**ECHOCARDIOGRAPHY AND DOPPLER IMAGING.** The echocardiographic measurements were performed according to a standard method published previously.<sup>21</sup> Briefly, mice were anesthetized using 2% to 3% isoflurane, with heart rate and body temperature continuously monitored. Transthoracic echocardiogram was performed at weeks 4 and 8 with a VisualSonics Vevo2100 40-MHz linear probe (Fujifilm VisualSonics Inc). LV ejection fraction (LVEF) and diastolic function were obtained in the parasternal long-axis view, with scans repeated thrice. Analyses were completed offline using the VisualSonics workstation (VevoLab). Global longitudinal strain (GLS) was determined using B-mode traces and analyzed with semiautomated VevoStrain software.

**ANIMAL TISSUE COLLECTION.** Following completion of the study, mice were sacrificed using pentobarbital (75 mg/kg) injected intraperitoneally, and organs were snap-frozen in liquid nitrogen and stored at -80 °C. Blood was collected into EDTA-coated tubes and centrifuged at 2,000 relative centrifugal force (rcf)

for 20 minutes at 4 °C, and the plasma stored at -80 °C. The length of the tibia was measured using a digital vernier caliper. Lungs were air-dried and weighed every 2 days until stable. Details on mitochondrial isolation and high-resolution respirometry procedures for cardiac tissues are available in the [Supplemental Appendix](#).

#### LIQUID CHROMATOGRAPHY-TANDEM MASS SPECTROMETRY.

Myocardial metabolites were extracted and determined using previously published methodology incorporating hydrophilic interaction liquid chromatography-tandem mass spectrometry (LC-MS/MS) using a 2.1 × 150-mm Atlantis hydrophilic interaction liquid chromatography column (Waters) in positive ion mode and a 2.1 × 100-mm bridged ethylsiloxane/silica hybrid particles that are bonded to the high-polarity amide groups (bridged ethyl-siloxane/silica hybrid amide) in negative ion mode.<sup>22,23</sup> Multiple reaction-monitoring transitions for all NAD metabolites were identified using analytical grade reference standards and MS/MS spectra with identified fragment structures, as previously reported.<sup>24</sup> Multidimensional data (retention time, *m/z*, and MS/MS transitions) was used to distinguish closely related metabolites, such as NAD<sup>+</sup> and the reduced form of nicotinamide adenine dinucleotide (NADH). Quantification of NR, NAD<sup>+</sup>, NADH, mitochondrial oxidized nicotinamide adenine dinucleotide phosphate (NADP<sup>+</sup>), and reduced form of nicotinamide adenine dinucleotide phosphate (NADPH) was performed based on standard curves with known concentrations of reference standards ranging from 50 nmol/L to 10 μmol/L.

#### SAMPLE PREPARATION FOR MASS SPECTROMETRY-BASED

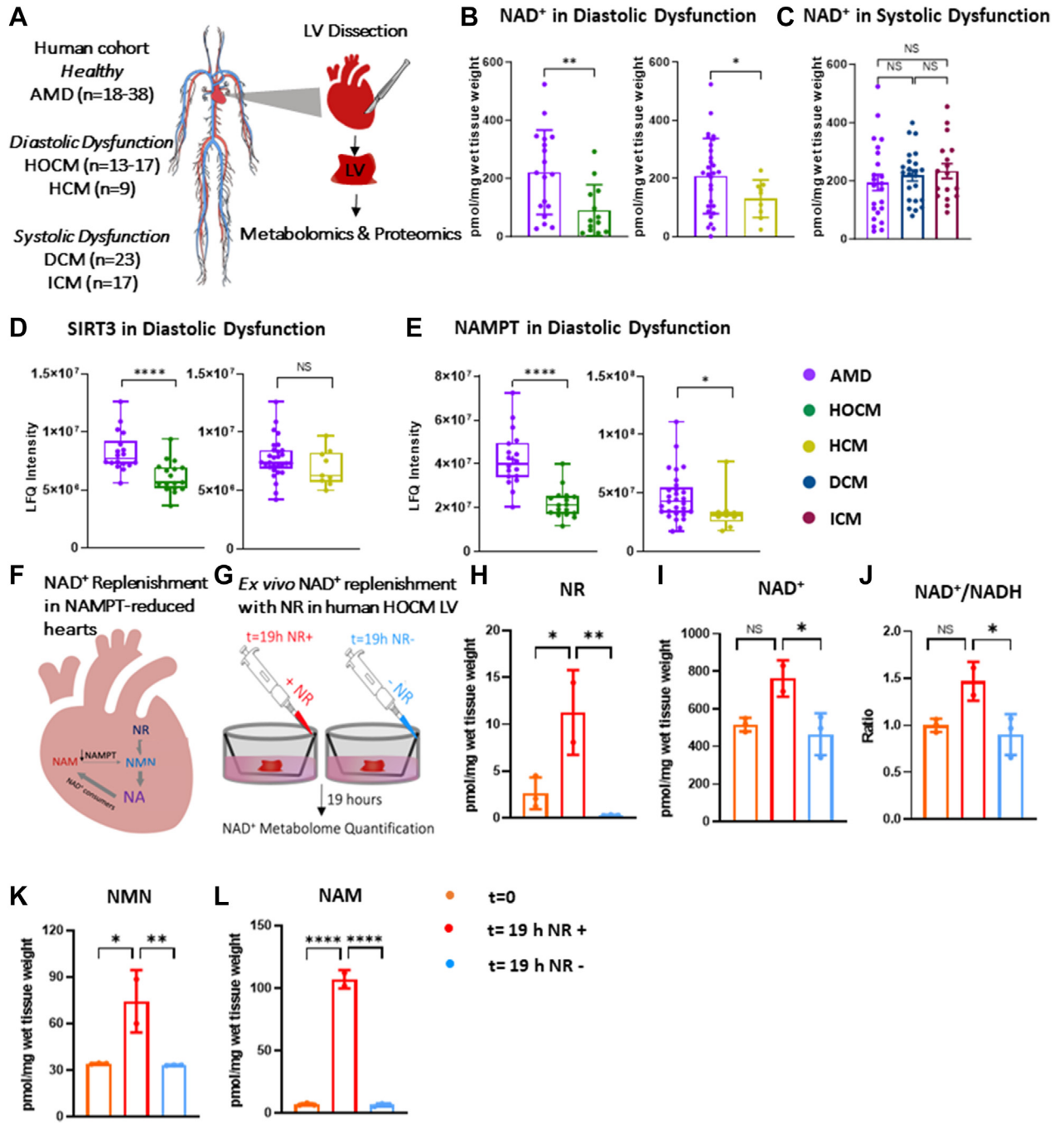
**PROTEOMICS.** Frozen heart tissue was powdered and weighed (~10 mg) into 2-mL microcentrifuge tubes and was homogenized in 100 μL of 4% sodium deoxycholate and 100 mmol/L Tris HCl (pH adjusted to 8). Tissue lysates were then heated at 95 °C and mixed at 1,000 revolutions/min for 10 minutes using Thermomixer C (Eppendorf) followed by centrifugation at 18,000 *g* for 10 minutes at room temperature. Next, 20 μg of protein from the tissue lysates (concentration determined by bicinchoninic acid assay) was subjected to simultaneous reduction and alkylation with tris(2-carboxyethyl)phosphine and chloroacetamide for 10 minutes at 95 °C and 1,000 revolutions/min in the Thermomixer C. Samples were then processed for trypsin digestion and subjected to a peptide cleanup.<sup>25</sup> Peptides were resuspended in 5% formic acid and stored at 4 °C until acquired by LC-MS.

**DATA-DEPENDENT MASS SPECTROMETRY-BASED PROTEOMICS.** Using a Thermo Fisher Dionex Ultimate

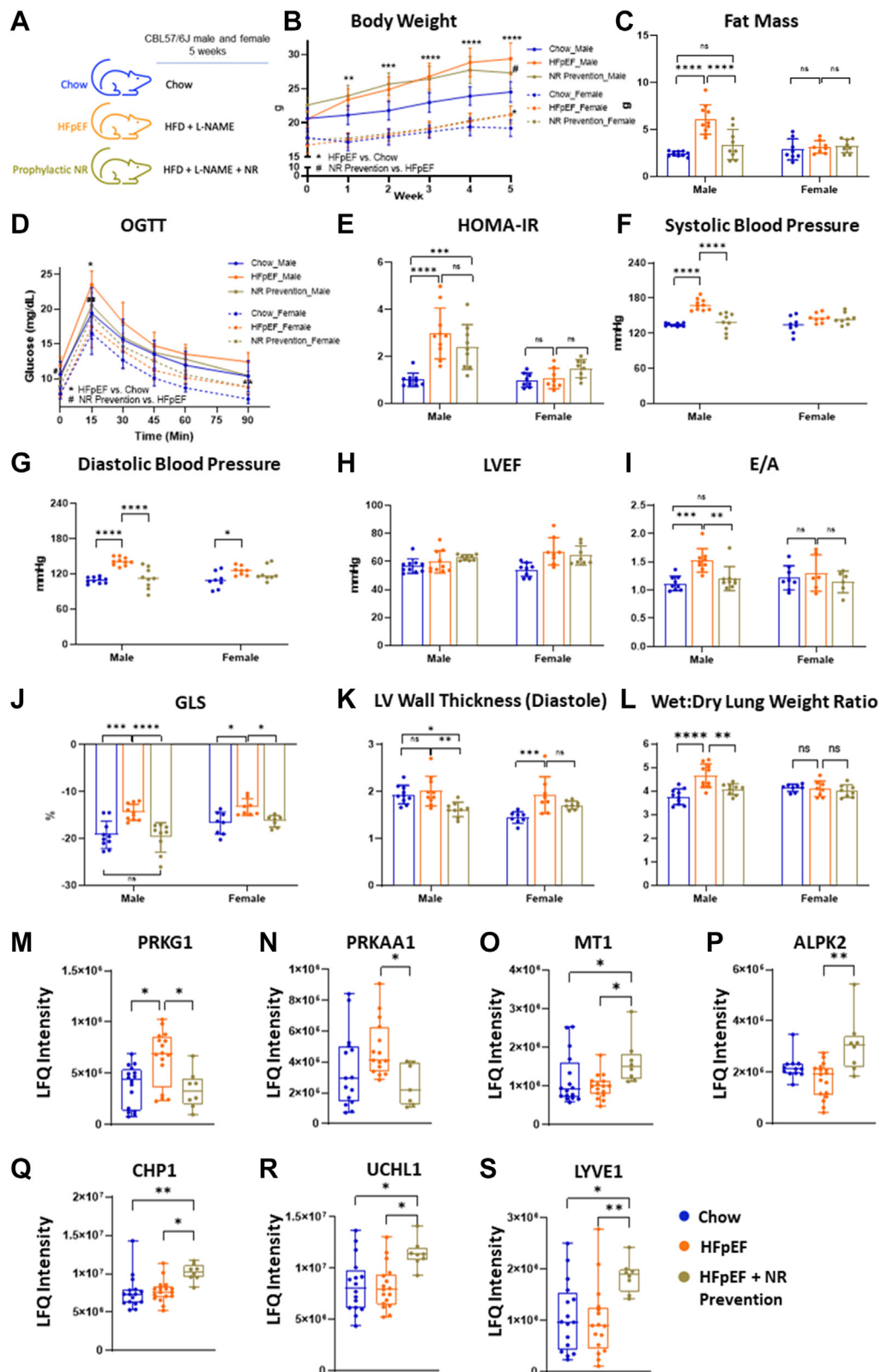
3000 ultra-high-performance liquid chromatography, peptides in 5% (volume/volume) formic acid (2 μg) were directly injected onto a 15-cm × 150-μm fused silica analytical column with an ~10-μm pulled tip containing C18 material (Dr Maisch; 1.9 μm, 130 Å), coupled online to a nanospray electrospray ionization source. Peptides were resolved over a gradient 5% to 40% acetonitrile over 50 minutes with a flow rate of 1,200 nL/min. Peptides were ionized by electrospray ionization at 2.4 kV. Tandem mass spectrometry analysis was carried out on a Thermo Exploris mass spectrometer using higher energy collisional dissociation fragmentation and a data-independent acquisition method as described previously.<sup>26</sup> The mass spectrometry-based proteomics data have been deposited to the ProteomeXchange Consortium via the PRoteomics IDentifications partner repository with the dataset identifier PXD033027 (username: reviewer\_pxd033027@ebi.ac.uk, password: 4vRe7-ZIM). Raw data were analyzed using the quantitative proteomics software DIA-NN<sup>27</sup> (version 1.7.16). Peptide and protein level identification were both set to a false discovery rate of 1% using a target-decoy-based strategy. The databases supplied to the search engine for peptide identifications contained both the mouse UniProt databases (Swissprot) downloaded on the May 7, 2021. A maximum of 1 missed cleavage by the protease trypsin was permitted. Oxidation of methionine (Met) was set as a variable modification. Carbamidomethyl on cysteine (Cys) was searched as a fixed modification.

**STATISTICS.** All graphical representations and statistical analyses were performed using GraphPad Prism version 9.5.1 for Windows (GraphPad Software). Metabolomics and proteomics data are presented using bar plots or boxplots based on the data distribution. Bar plots illustrate the mean ± SD for normally distributed data. Boxplots are presented for skewed data centered on the median with upper and lower quartiles indicated by the box boundaries. Comparisons between 2 groups were performed using Student's *t*-test or Mann-Whitney *U* test, depending on the distribution of the data. For experiments involving multiple groups, differences were analyzed using 1-way analysis of variance, and the Kruskal-Wallis test was used if the normality test (Shapiro-Wilk normality test) failed. The Tukey or Dunn post hoc test was used for multiple pairwise comparisons. For longitudinal data, 2-way repeated-measures analysis of variance was used with the Sidak post hoc test for multiple pairwise comparisons. A *P* value of <0.05 was considered statistically significant.

**FIGURE 1** NAD<sup>+</sup> Depletion in Human Diastolic Dysfunction Myocardium and Repletion With NR



(A) A schematic diagram of obtaining LV myocardium from the human cohort. (B, C) NAD<sup>+</sup> levels in human LV myocardium of (B) HOCM (n = 13) and HCM (n = 9) and (C) DCM (n = 23) and ICM (n = 17) when compared to AMD myocardium (n = 23). (D) Expression levels of SIRT3, an NAD<sup>+</sup>-consuming enzyme, in HOCM (n = 17) and HCM (n = 9) myocardium compared to AMD myocardium (n = 16-29). (E) Expression levels of NAMPT, the rate-limiting enzyme in NAD synthesis through the salvage pathway, in HOCM (n = 17) and HCM (n = 9) LV myocardium compared with AMDs (n = 18-29). (F) Schematic summary of the NAD<sup>+</sup> salvage pathway showing lower NAMPT levels in LV diastolic dysfunction myocardium. (G) Schematic overview of the myocardial slice model used to study NAD<sup>+</sup> replenishment using exogenous NR in HOCM LV. (H to L) Exogenous NR significantly elevated levels of myocardial (H) NR, (I) NAD<sup>+</sup>, (J) NAD<sup>+</sup>/NADH ratio, (K) NMN, and (L) NAM at time 0 (n = 3), 19 hours with NR<sup>+</sup> incubation (n = 2), and 19 hours of no NR control (n = 3), respectively. \*P < 0.05, \*\*P < 0.01, and \*\*\*P < 0.001 by (B) Student's *t*-test or (C, H to L) 1-way ANOVA followed by the Tukey test or (D, E) by the Mann-Whitney 2-sided test. AMD = age-matched donor; ANOVA = analysis of variance; DCM = dilated cardiomyopathy; HCM = hypertrophic cardiomyopathy; HOCM = hypertrophic obstructive cardiomyopathy; ICM = ischemic cardiomyopathy; LFQ = label-free quantitation; LV = left ventricular; NAD = nicotinamide adenine dinucleotide; NAD<sup>+</sup> = oxidized nicotinamide adenine dinucleotide; NADH = reduced form of nicotinamide adenine dinucleotide; NAM = nicotinamide; NAMPT = nicotinamide phosphoribosyltransferase; NMN = nicotinamide mononucleotide; NR = nicotinamide riboside; NS = not significant; SIRT3 = sirtuin 3.

**FIGURE 2** Prophylactic NR Averts HFpEF With Widespread Salutary Effects on Proteins Involved in Diastolic Homeostasis

Continued on the next page

## RESULTS

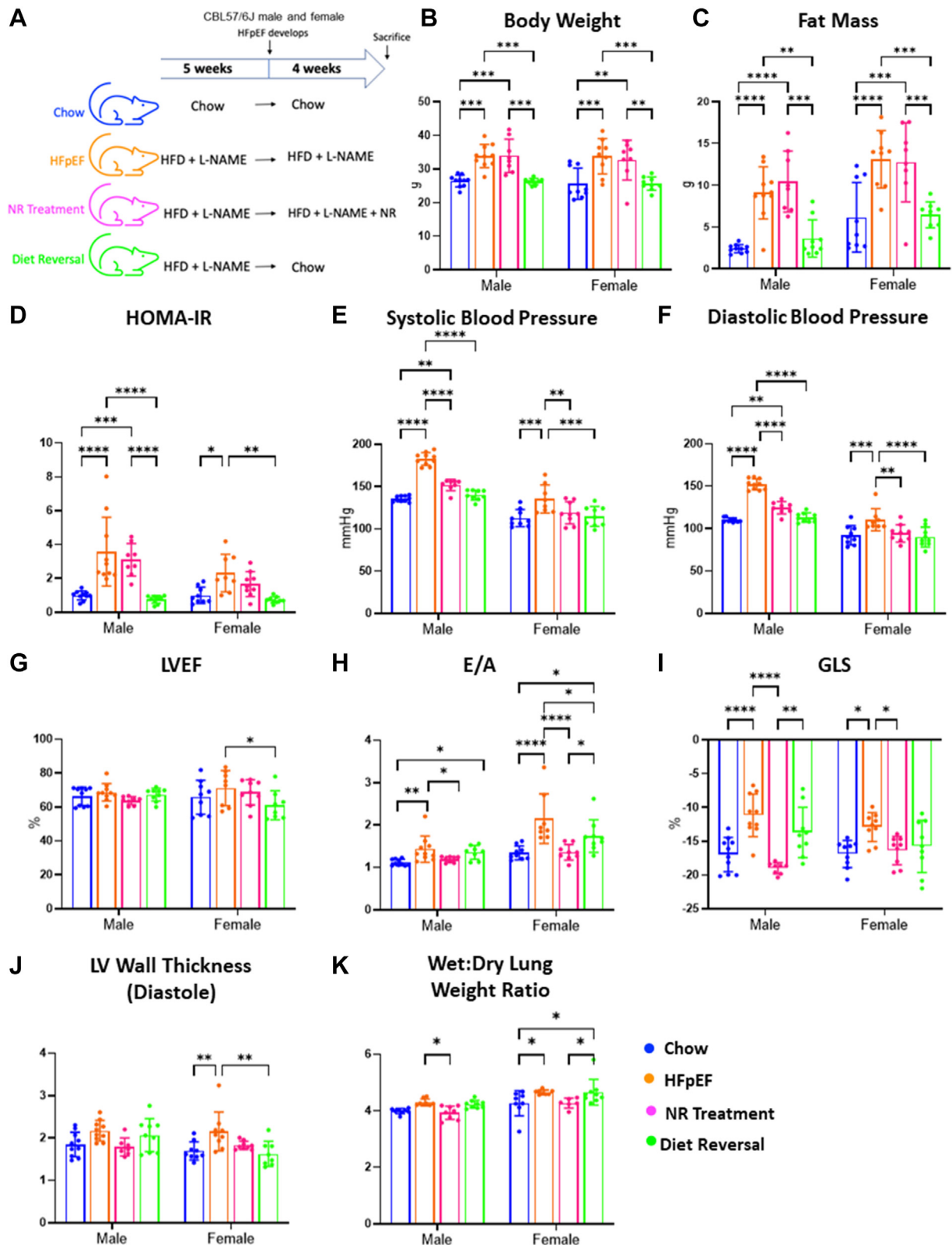
**NAD<sup>+</sup> DEPLETION IN HUMAN LV MYOCARDIUM WITH DIASTOLIC DYSFUNCTION AND REPLETION WITH NR.** Pathologic LV hypertrophy is synonymous with diastolic dysfunction, so we examined NAD<sup>+</sup> levels in 2 hypertrophic cardiomyopathies (HOCM and HCM) and 2 types of HF with systolic impairment (DCM and ICM) (Figure 1A). We found a significant depletion of NAD<sup>+</sup> in LV myocardium from patients with HOCM and HCM myocardium (Figure 1B) compared to age-matched donor (AMD) (histologically normal donor LV) myocardium. However, in ICM and DCM, the 2 most common forms of HF with reduced ejection fraction (characterized by predominant systolic impairment), NAD<sup>+</sup> levels were comparable to those in AMDs (Figure 1C). We also saw significant reduction in the expression of sirtuin 3 (SIRT3), an NAD<sup>+</sup>-consuming enzyme, in HOCM and nonsignificant reduction in HCM (Figure 1D) LV myocardium. The rate-limiting enzyme in NAD<sup>+</sup> metabolism, NAMPT, was significantly lower in HOCM and HCM myocardium (Figure 1E). Expression levels of SIRT3 and NAMPT proteins were lower in DCM but not in ICM LV myocardium when compared to AMDs (Supplemental Figures 1A and 1B). Using a novel ex vivo myocardial tissue slice model<sup>28</sup> (Figures 1F and 1G), we then showed that in human HOCM LV myocardium, exogenous NR significantly elevated tissue NR (Figure 1H), NAD<sup>+</sup> (Figure 1I), NAD<sup>+</sup>/NADH ratio (Figure 1J), nicotinamide mononucleotide (Figure 1K), and nicotinamide (Figure 1L) after NR incubation at 37 °C in a 5% CO<sub>2</sub> humidified atmosphere. These results demonstrate that exogenous NR can be taken up by the diseased human heart

to replenish NAD<sup>+</sup>, notwithstanding NAMPT depletion. This prompted us to study the relationship of myocardial NAD<sup>+</sup> depletion and diastolic impairment, with a focus on HFpEF, the commonest manifestation and most clinically relevant presentation of diastolic dysfunction,<sup>29</sup> in a recently established murine HFpEF model.<sup>3</sup>

**PROPHYLACTIC NR AVERTS HFpEF WITH WIDESPREAD SALUTARY EFFECTS ON PROTEINS INVOLVED IN MAINTAINING DIASTOLIC HOMEOSTASIS.** In this experimental model, 5 weeks of HFD and L-NAME in drinking water (Figure 2A) resulted in substantial alterations in several metabolic parameters in male mice. These included increased body weight (Figure 2B), fat mass (Figure 2C), glucose excursion measured by oral glucose tolerance test (Figure 2D), insulin resistance (homeostatic model assessment of insulin resistance [HOMA-IR]) (Figure 2E), and systolic and diastolic blood pressures (Figures 2F and 2G). The same levels of change was not observed in female mice in the same timeframe. Maintaining normal systolic function, as indicated by an unchanged LVEF (Figure 2H), the male mice showed a significant increase in transmitral Doppler early to late diastolic transmitral flow velocity (E/A) wave ratio (Figure 2I), indicating diastolic dysfunction, a hallmark of HFpEF. Such changes were not significantly observed in female mice. Both sexes demonstrated reduced GLS (Figure 2J), suggesting diastolic impairment. Interestingly, although LV wall thickness in male mice remained largely unchanged, it increased significantly in female mice (Figure 2K). The wet/dry lung ratio, a marker for congestive HF, showed an increase only in male mice (Figure 2J).

### FIGURE 2 Continued

(A) Schematic overview of the feeding protocol. (B) Weekly body weight starting at week 0 of the diet, (C) fat mass (D) glucose response curve during OGTT, and (E) HOMA-IR of male and female mice of the chow, HFpEF, and NR prevention groups at week 4. (F) Systolic and (G) diastolic blood pressures of male and female mice of the chow, HFpEF, and NR prevention groups obtained by a noninvasive blood pressure monitoring method at week 5. (H) LVEF, (I) E/A ratio, (J) GLS, and (K) wall thickness of the chow, HFpEF and NR prevention groups of male and female mice measured by echocardiography. (L) Wet/dry ratio of the lung weight of male and female mice of the HFpEF and NR prevention groups at week 5 (n = 8-10/group for chow, HFpEF, and prophylactic NR male mice; n = 6-8/group for chow, HFpEF, prophylactic NR female mice). Expression levels of (M) protein kinase G (PRKG1), (N) protein kinase AMP-activated catalytic subunit alpha 1 (PRKAA1), (O) metallothionein 1 (MT1), (P) alpha-protein kinase 2 (ALPK2), (Q) calcium-binding protein 1 (CHP1), (R) ubiquitin carboxyl-terminal hydrolase isozyme L1 precursor (UCHL1), and (S) lymphatic vessel endothelial hyaluronic acid receptor 1 (LYVE1) in myocardium of chow (n = 12-16), HFpEF (n = 15-17), and NR prevention (n = 7 or 8) groups after 5 weeks of chow, HFD + N<sup>[w]</sup>-nitro-L-arginine methyl ester (L-NAME), and NR + HFD + L-NAME diet. Each point represents a mouse. \*P < 0.05, \*\*P < 0.01, and \*\*\*P < 0.001 by (B, D) 2-way repeated-measures ANOVA followed by the Sidak posttest, (C, E to L) 2-way ANOVA followed by the Sidak multiple comparisons test or (M to S) the Kruskal-Wallis test followed by Dunn multiple comparison testing. AMP = adenosine monophosphate; E/A = transmitral Doppler E- to A-wave ratio; GLS = global longitudinal strain; HFD = high-fat diet; HFpEF = heart failure with preserved ejection fraction; HOMA-IR = homeostatic model assessment of insulin resistance; LVEF = left ventricular ejection fraction; OGTT = oral glucose tolerance test; other abbreviations as in Figure 1.

**FIGURE 3** NR Therapy Fully Rescues HFpEF, and Dietary Intervention Partially Rescues HFpEF

Continued on the next page

Prophylactic supplementation of NR in concert with HFD and L-NAME averted the metabolic, hypertensive, and cardiac perturbations of HFpEF in male, but not female, mice (Figures 2B to 2L). It prevented weight gain (Figure 2B), fat mass accumulation (Figure 2C), abnormal glucose excursion during oral glucose tolerance test (Figure 2D) (although not HOMA-IR [Figure 2E]), and systolic (Figure 2F) and diastolic (Figure 2G) hypertension. As expected, there was no change in LVEF (Figure 2H). There were significant improvements in E/A ratio (Figure 2I), GLS (Figure 2J), LV wall thickness (Figure 2K), and wet/dry lung ratio (Figure 2L). GLS was the only parameter also significantly improved in the female prophylactic NR therapy mice (Figure 2J).

We proceeded to examine underlying molecular changes in myocardium from prophylactic NR male mice to examine the myocardial molecular differences in these mice compared to the mice exhibiting HFpEF. The prophylactic NR group displayed distinct myocardial protein alterations, measured using LC-MS/MS proteomics, when compared to the HFpEF group, as shown in the volcano plot in Supplemental Figure 2A. Protein kinase CGMP-dependent 1 (PRKG1), a protein previously shown to exacerbate stress-induced cardiomyopathy,<sup>30</sup> was significantly up-regulated in HFpEF but remained at control levels in NR-prevention myocardium (Figure 2M). Protein kinase adenosine monophosphate-activated catalytic subunit alpha 1 (PRKAA1), a key component of the adenosine monophosphate-activated protein kinase complex critical for intracellular energy sensing and regulation, was significantly decreased in prophylactic NR myocardium compared to HFpEF (Figure 2N).

Prophylactic NR treatment led to a heightened expression of metallothionein 1 (MT1) (Figure 2O), a protein that is known to play a crucial role in mitigating myocardial inflammation and supporting remodeling in cardiomyopathy.<sup>31</sup> Simultaneously, there was a significant increase in the expression of

alpha protein kinase 2 (ALPK2) within the myocardium of the prophylactic NR group (Figure 2P), a protein known to promote cardiogenesis through wingless/integrated signaling suppression in both zebrafish and human pluripotent stem cells,<sup>32</sup> which may serve as a compensatory mechanism in response to the nonsignificant decrease observed in HFpEF myocardium.

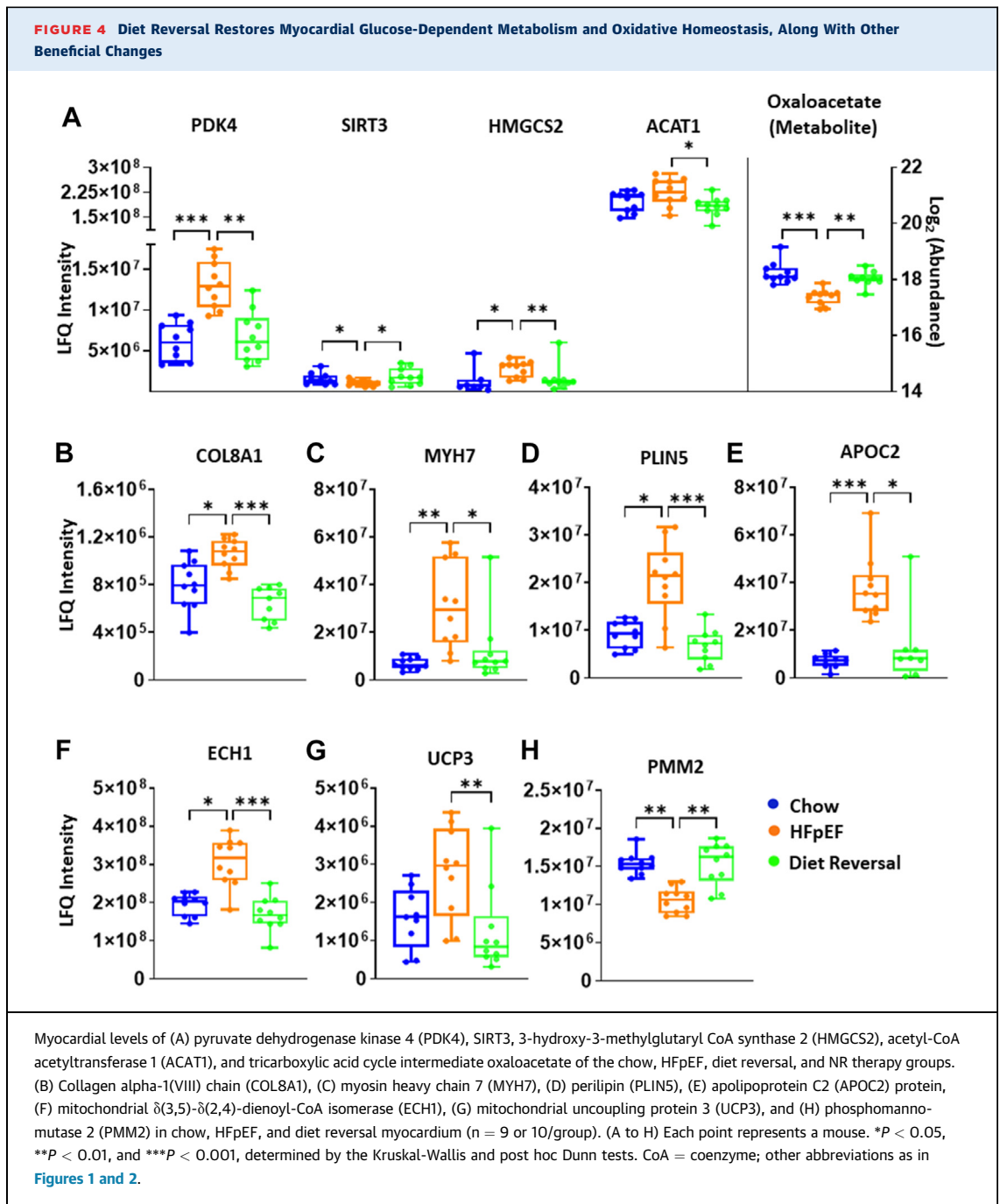
Calcineurin homologous protein 1 (CHP1), an essential component of the Na<sup>+</sup>/H<sup>+</sup> exchanger family, was significantly increased in prophylactic NR myocardium (Figure 2Q).<sup>33</sup> Another protein, ubiquitin C-terminal hydrolase L1 (UCHL1), known for its involvement in postinfarct fibrosis<sup>34</sup> and contributing to pathologic cardiac hypertrophy through the stabilization of the epidermal growth factor receptor,<sup>35</sup> was significantly elevated in prophylactic NR myocardium (Figure 2R). Lymphatic vessel endothelial hyaluronic acid receptor 1 (LYVE1), a protein critical for lymphangiogenesis and cardiac functionality,<sup>36</sup> was significantly increased in prophylactic NR myocardium compared to chow and HFpEF (Figure 2S).

**NR THERAPY FULLY RESCUES HFpEF; DIET REVERSAL PARTIALLY RESCUES HFpEF.**

After 9 weeks of the HFD + L-NAME protocol (Figure 3A), significant elevation of body weight was observed in both male and female mice (Figure 3B). The diet reversal group had replacement of HFD + L-NAME with normal chow, and L-NAME was removed from the drinking water at the 5-week mark. Upon reassessment at the 9-week mark, the diet reversal group demonstrated a significant reduction in body weight (Figure 3B) and fat mass (Figure 3C) as compared to both the HFpEF and NR therapy groups. In both sexes, increases in body weight and fat mass were not mitigated by NR therapy, with measurements remaining comparable to those observed in the HFpEF group (Figures 3B and 3C). The HFpEF group had significantly impaired HOMA-IR, which was not

**FIGURE 3 Continued**

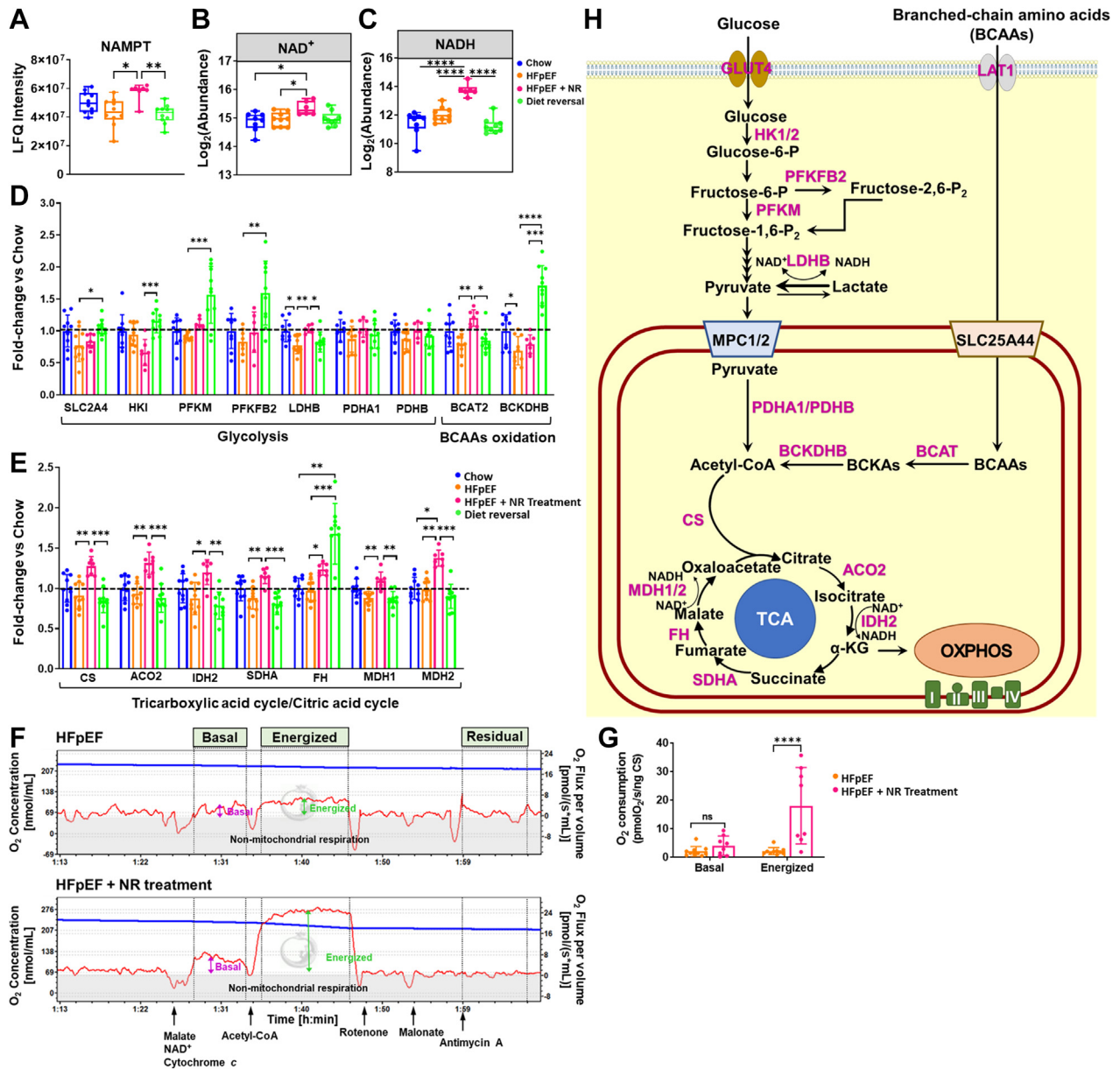
(A) A schematic overview of NR therapy and reverse diet feeding protocol after full development of HFpEF. (B) Body weight, (C) fat mass, and (D) HOMA-IR of both male and female mice of the chow, HFpEF, NR therapy, and diet reversal groups at the end of study. (E) Systolic and (F) diastolic blood pressures of both male and female mice after 4 weeks of chow, HFD + L-NAME (HFpEF), NR supplementation, or reverse dieting. (G) LVEF, (H) E/A ratio, (I) GLS, (J) LV wall thickness, (K) wet/dry lung weight ratio of both male and female of chow, HFpEF, NR therapy, and diet reversal groups at the end of study (n = 7-10/group for chow, HFpEF, NR therapy, and diet reversal male mice (n = 8 or 9/group for chow, HFpEF, NR therapy, and diet reversal female mice). Each point represents a mouse. (B to K) All data are presented as the mean ± SD. \*P < 0.05, \*\*P < 0.01, and \*\*\*P < 0.001 by 2-way ANOVA followed by the Sidak multiple comparisons test. Abbreviations as in Figures 1 and 2.



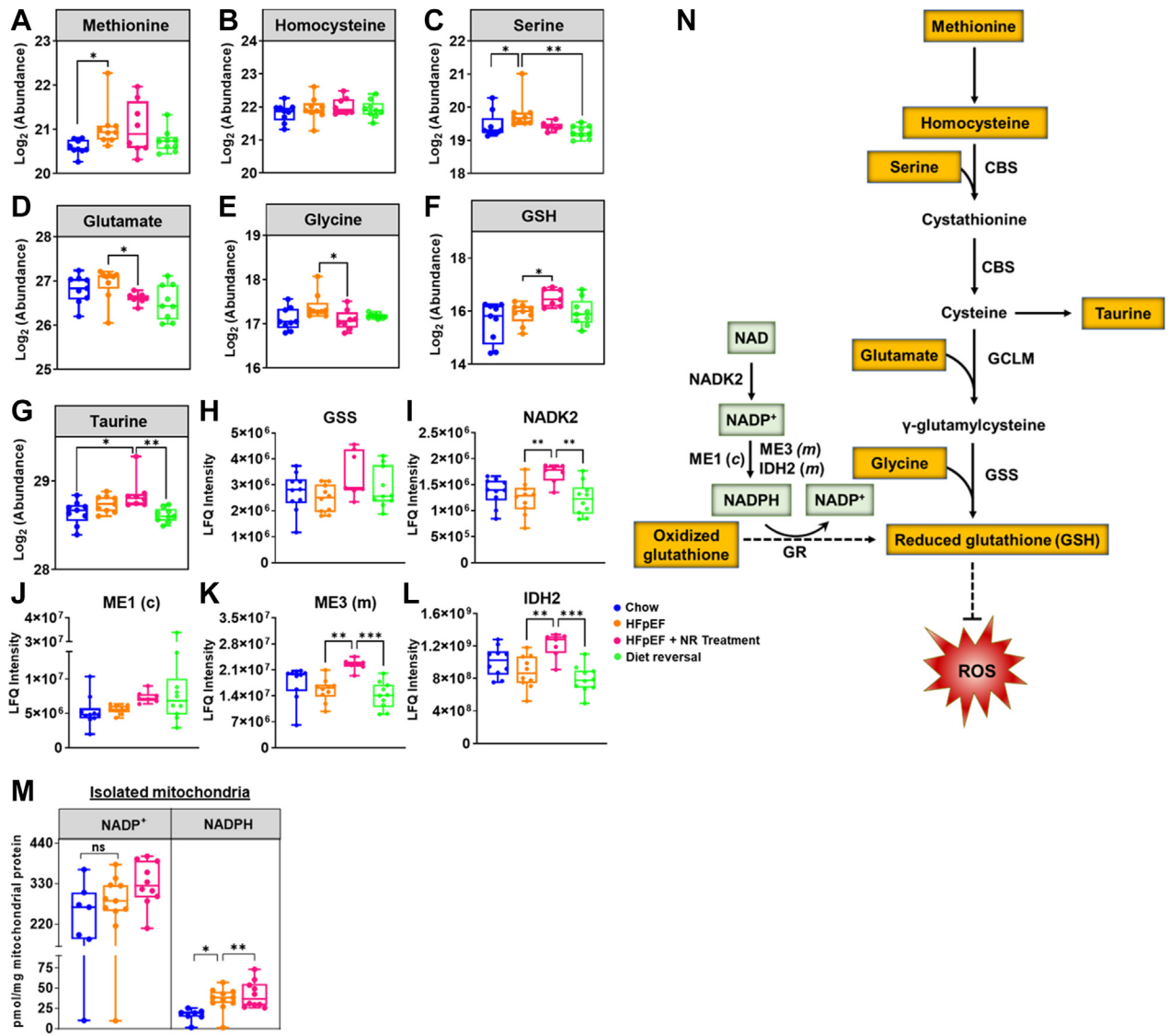
changed with NR therapy; however, diet reversal improved HOMA-IR similar to that in the chow group (Figure 3D) in both male and female mice. The diet reversal and NR therapy groups resulted in significant reductions in systolic (Figure 3E) and diastolic (Figure 3F) blood pressures in both male and female mice, without an effect on LVEF (Figure 3G) in males, but a subtle decrease in LVEF was observed in diet

reversal female mice. NR therapy, but not diet reversal, significantly improved LV diastolic function as determined by E/A wave ratio (Figure 3H) in mice of both sexes and GLS (Figure 3I) in male mice compared to HFpEF. Diet reversal, but not NR, significantly reduced LV wall thickness (Figure 3J) in females, and NR decreased wet/dry lung weight ratio (Figure 3K) in mice of both sexes, but diet reversal did not.

**FIGURE 5 NR Treatment Increases NAD<sup>+</sup> Bioavailability and Mediates Metabolic Reprogramming to Improve Cardiac Energy Homeostasis in HFpEF**



(A) NAMPT protein expression levels, and both (B) NAD<sup>+</sup> and (C) NADH levels in the myocardium of chow (n = 8-10), HFpEF (n = 9 or 10), NR-treated HFpEF (n = 6 or 7), and diet reversal mice (n = 9). (D) Protein expression levels of solute carrier family 2 member 4 (SLC2A4)/glucose transporter 4 (GLUT4); mitochondrial hexokinase (HK1); phosphofructokinase, muscle (PFKM); phosphofructokinase (PFKFB2); lactate dehydrogenase B chain (LDHB); pyruvate dehydrogenase E1 component subunit alpha (PDHA1); pyruvate dehydrogenase component subunit beta (PDHB); and branched chain amino acid transaminase 2 (BCAT2) and 2-oxoisovalerate dehydrogenase subunit beta, mitochondrial (BCKDHB) in chow, HFpEF, NR-treated HFpEF, and diet reversal myocardium (n = 7-10/group). (E) Protein expression levels of citrate synthase (CS), mitochondrial aconitase 2 (ACO2), mitochondrial isocitrate dehydrogenase [NADP<sup>+</sup>] 2 (IDH2), succinate dehydrogenase complex flavoprotein subunit A (SDHA), fumarate hydratase (FH), cytoplasmic malate dehydrogenase (MDH1), and mitochondrial malate dehydrogenase (MDH2) in the myocardium of chow, HFpEF, NR-treated HFpEF, and diet reversal mice (n = 7-10/group). (F) Representative trace of respirometric measurement of HFpEF and NR-treated HFpEF hearts as described in the Methods section. Experimental trace recorded by Oxygraph-2k (Oroboros) with from acquisition software DatLab4.3 (Oroboros Instruments) showing the actual O<sub>2</sub> concentration (blue, left y-axis in nmol/mL) and rate of oxygen consumption (red, right y-axis in pmol O<sub>2</sub>/s/mL). Sequential additions of substrates and inhibitors are marked by arrows and abbreviations below the trace (malate: 2 mmol/L; NAD<sup>+</sup>: 100 μmol/L; cytochrome c: 10 μmol/L; acetyl-CoA 150 μmol/L; rotenone: 1 μmol/L; malonate: 5 mmol/L; antimycin A: 2.5 μmol/L). Vertical dotted lines denote the actual respiratory state after the addition of malate, NAD<sup>+</sup>, and cytochrome c (basal), acetyl-CoA (energized) and antimycin A (residual) states. (G) Oxygen consumption rates in the energized state of HFpEF (n = 10) and NR-treated mice (n = 8). The rates of O<sub>2</sub> consumption in the residual state were subtracted from basal and energized rates and were normalized to citrate synthase (CS) protein. (H) A schematic illustrating the locations and functions of the proteins in C and D. \*P < 0.05, \*\*P < 0.01, and \*\*\*P < 0.001 by (A to C) the Kruskal-Wallis test followed by the Dunn multiple comparison test, (D, E) 1-way ANOVA, or (G) 2-way ANOVA with Sidak multiple comparison. NADP<sup>+</sup> = oxidized form of nicotinamide adenine dinucleotide phosphate; OXPHOS = oxidative phosphorylation; TCA = tricarboxylic acid; other abbreviations as in Figures 1 and 2.

**FIGURE 6 NR Therapy, But Not Diet Reversal, Increases Antioxidant Protection in HFpEF Myocardium**

NR increased the generation of NADPH and the synthesis of reduced glutathione (GSH) 9 methionine-fueled transsulfuration. Metabolite levels of (A) methionine; (B) homocysteine; and amino acids, including (C) serine, (D) glutamate, (E) glycine, (F) GSH, and (G) taurine in chow, HFpEF, NR-treated, and diet reversal hearts are presented using boxplots. Protein expression levels of (H) glutathione synthase (GSS); (I) NAD kinase (NADK2), the only enzyme that phosphorylates NAD<sup>+</sup> into NADP; both cytosolic malic enzymes (ME) (J) ME1 and (K) ME3; and (L) mitochondrial isozymes of IDH, IDH2, in chow, HFpEF, NR-treated, and diet reversal hearts are also depicted using boxplots (n = 7-10/group). (M) NADP<sup>+</sup>, NADPH, and NADP<sup>+</sup>/NADPH ratio in mitochondria isolated from the hearts of chow (n = 7), HFpEF (n = 11) and NR-treated myocardium (n = 10). (N) A schematic summarizing the changes in intermediates leading to increased production of NADPH-GSH. \*P < 0.05, \*\*P < 0.01, and \*\*\*P < 0.001 by the Kruskal-Wallis test followed by the Dunn multiple comparison test. c = cytosolic; CBS = cystathionine beta-synthase; GCLM = glutamate-cysteine ligase modifier; GR = glutathione reductase; m = mitochondrial; NADPH = reduced form of nicotinamide adenine dinucleotide phosphate; ROS = reactive oxygen species; other abbreviations as in [Figures 1, 2, and 5](#).

**DIET REVERSAL RESTORES MYOCARDIAL GLUCOSE-DEPENDENT METABOLIC PATHWAYS, ALONG WITH OTHER BENEFICIAL CHANGES.** We proceeded to examine underlying molecular changes in myocardium from chow, HFpEF, NR therapy, and diet

reversal male mice. Consistent with enhanced insulin sensitivity in the diet reversal group, even though LV diastolic functional parameters did not significantly improve within the observed timeframe, there were protein and metabolite changes suggesting the

reactivation of glucose-dependent metabolism. The volcano plot in [Supplemental Figure 2B](#) demonstrates the unique differences in myocardial protein expression between the diet reversal and HFpEF groups. For example, pyruvate dehydrogenase kinase 4 (PDK4), which suppresses glucose oxidation and is linked to insulin resistance, was up-regulated in HFpEF myocardium ([Figure 4A](#)); remarkably, diet reversal induced complete resolution of PDK4 levels, suggesting augmented insulin sensitivity. For ease of interpretation, the glycolytic and tricarboxylic acid (TCA) cycle enzyme changes are grouped in [Figure 5](#) alongside an enabling schematic. The insulin-regulated glucose transporter found in striated muscle, GLUT4, encoded by the solute carrier 2A4 (*Slc2a4*) gene, was significantly up-regulated in these hearts compared to HFpEF ([Figure 5D](#)). Hexokinase I, the rate-limiting enzyme that initiates the first step of glycolysis by phosphorylating intracellular glucose into glucose 6-phosphate, was shown to reduce in HFpEF hearts, but there were no changes in Hexokinase-1 expression in NR-treated HFpEF. Hexokinase-1 was significantly up-regulated in diet reversal myocardium ([Figure 5D](#)), supporting restoration of the HK1-dependent glycolysis pathway in diet reversal mice compared to NR-treated HFpEF mice. Diet reversal myocardium had significantly elevated levels of phosphofructokinase (PFKM) ([Figure 5D](#)), an enzyme that catalyzes the phosphorylation of D-fructose-6-phosphate to fructose-1,6-bisphosphate, enabling procession through glycolysis to pyruvate. Oxaloacetate, an intermediate metabolite in the TCA cycle, was suppressed in HFpEF myocardium but recovered to normal levels by diet reversal ([Figure 4A](#)), suggesting recovery of pyruvate output and normalized flux of the TCA cycle.

SIRT3, an NAD<sup>+</sup>-dependent enzyme, was significantly depleted in HFpEF myocardium, but in diet reversal myocardium it was comparable to control levels ([Figure 4A](#)), illustrating recovery of this important mediator of salutary posttranscriptional effects. Intriguingly, levels of 3-hydroxy-3-methylglutaryl-coenzyme A synthase 2 (HMGCS2), the canonical ketogenic enzyme, were significantly elevated in HFpEF myocardium and recovered to normal levels in diet reversal myocardium ([Figure 4A](#)). This likely represents the abundance of acetyl-CoA delivered from fatty acid metabolism that serves as a ketogenic shuttle in HFpEF myocardium; with the removal of HFD, restoration of glycolysis,

and increased generation of oxaloacetate, fatty acids are no longer diverted to ketone generation. Acetyl-CoA acetyltransferase 1 (ACAT1) was significantly reduced in diet reversal myocardium compared to HFpEF myocardium ([Figure 4A](#)), which is colinear with the HMGCS2 response.

There were many other changes at the protein level indicative of salutary effects. For example, collagen 8 type A protein (COL8A1), a protein linked to cardiac dilation and remodeling in human DCM,<sup>37</sup> was up-regulated in HFpEF myocardium but returned to chow levels by diet reversal ([Figure 4B](#)). Levels of  $\beta$ -myosin heavy chain 7 (MYH7) were significantly increased in HFpEF myocardium, possibly because of hypertensive remodeling, but returned to control levels in diet reversal myocardium ([Figure 4C](#)), suggesting a remodeling capability of myocardium's key structural proteins when metabolic and hypertensive stressors are removed.

Following dietary intervention, changes were observed in proteins involved in lipid metabolism. The intramyocellular lipid contributor perilipin 5 (PLIN5), initially elevated in HFpEF myocardium, was normalized ([Figure 4D](#)). Apolipoprotein 2 (APOC2), which assists in exporting excess toxic lipid species, was initially higher in HFpEF myocardium but reduced to control levels ([Figure 4E](#)). Also,  $\delta(3,5)$ - $\delta(2,4)$ -dienoyl-CoA isomerase (ECH1), a crucial player in fatty acid oxidation, and mitochondrial uncoupling protein 3 (UCP3), which aids in fatty acid-response oxidative phosphorylation, were initially elevated in HFpEF myocardium but normalized with diet reversal ([Figures 4F and 4G](#)). Phosphomannomutase 2 (PMM2), involved in nucleotide-sugar biosynthesis, was significantly down-regulated in HFpEF myocardium and resolved to control levels in diet reversal myocardium ([Figure 4H](#)).

#### **THERAPEUTIC RECOVERY OF NAD<sup>+</sup> UP-REGULATES LACTATE, BRANCHED-CHAIN AMINO ACID METABOLISM, AND TCA FLUX.**

NR therapy after the establishment of HFpEF significantly increased expression of NAMPT ([Figure 5A](#)) along with levels of NAD<sup>+</sup> ([Figure 5B](#)) and NADH ([Figure 5C](#)). Unlike diet reversal, NR treatment did not improve insulin resistance and glucose metabolism. NR did not increase protein expression of enzymes that facilitate the metabolism of glucose, including insulin-responsive glucose transporter GLUT4, HK1, PFKM, and PFKFB2 enzymes that catalyze the phosphorylation of glucose ([Figure 5D](#)). However, NR increased

lactate dehydrogenase B (LDHB) (Figure 5D), a critical isoform of LDH enzyme that has higher affinity for lactate and can increase pyruvate supply by preferentially converting lactate to pyruvate, thereby directing it toward the TCA cycle for further energy production. Together, these highlight potential rescue pathways during insulin resistance and glucose insufficiency. In addition, we also found elevated expression of mitochondrial branched-chain amino acid transaminase 2 (BCAT2) and nonsignificant increase in branched-chain keto acid dehydrogenase E1 subunit beta (BCKDHB) (Figure 5D) proteins in myocardium from NR-treated mice compared to HFpEF mice.

Additionally, NR treatment led to an elevation of several TCA cycle-associated enzymes, including citrate synthase (CS); aconitase 2 (ACO2); succinate dehydrogenase complex, subunit A (SDHA); fumarate hydratase (FH); and 3 rate-limiting TCA enzymes that serve to generate NADH: isocitrate dehydrogenase regulatory subunit 3 (IDH3), along with malate dehydrogenase 1 and 2 (MDH1, MDH2) (Figure 5E). As an electron donor, NADH produced in the TCA cycle plays a crucial role in adenosine triphosphate (ATP) synthesis by oxidative phosphorylation, which generates most of its energy through the electron transport chain (Figure 5H). Corresponding box plots and cluster heatmap of proteins in Figures 5D and 5E are presented Supplemental Figures 3 and 4.

To investigate whether NR supplementation improves mitochondrial respiration function in HFpEF mice, we measured mitochondrial respiratory capacity in HFpEF and NR-treated HFpEF mice using the Oroboros Oxygraph-2k based on the previously published protocol by Zuccolotto-dos-Reis et al.<sup>38</sup> Oxygen consumption rates in the energized state were found to be significantly higher in the NR-treated HFpEF mouse hearts as compared with HFpEF mouse hearts (Figures 5F and 5G), suggesting an increased mitochondrial respiration rate and ATP generation in HFpEF mice treated with NR.

**THERAPEUTIC NR SUPPLEMENTATION ENHANCES ANTIOXIDANT CAPACITY BY MODULATING LEVELS OF THE REDUCED FORM OF NICOTINAMIDE ADENINE DINUCLEOTIDE PHOSPHATE AND GLUTATHIONE.** NAD<sup>+</sup> replenishment via NR therapy also appeared to enhance antioxidant capacity in the myocardium via reduced form of nicotinamide adenine dinucleotide phosphate mediated regeneration of reduced glutathione (GSH). Redistribution of homocysteine flux

between the transmethylation and transsulfuration pathways plays a significant role in facilitating GSH synthesis. Although no change was detected in the levels of methionine, homocysteine, and serine (Figures 6A to 6C), the NR-treated myocardium exhibited a significant reduction in glutamate (Figure 6D) but not in glycine levels (Figure 6E) relative to HFpEF mice. These alterations suggest their potential involvement in GSH biosynthesis. Additionally, when cysteine availability surpasses the demand for GSH synthesis, the excess cysteine is metabolized into taurine (Figure 6G). An increase in GSH (Figure 6F) levels was observed, accompanied by a nonsignificant increase in the expression of glutathione synthetase (GSS) (Figure 6H). NAD kinase 2, mitochondrial (NADK2), which catalyzes phosphorylation of NAD to generate NADP<sup>+</sup>, was significantly increased in NR therapy myocardium (Figure 6I). NADP<sup>+</sup> can be reduced to NADPH by NADP-dependent malic enzyme 1 (ME1) in the cytoplasm and by ME3 and isocitrate dehydrogenase 2, mitochondrial (IDH2) in the mitochondria,<sup>39</sup> the latter 2 of which were significantly higher in myocardium from NR-treated vs nontreated HFpEF mice (Figures 6K and 6L). In isolated mitochondria, we found a 1.4-fold increase in NADP<sup>+</sup> ( $P = 0.06$ ) in NR therapy myocardium and a 2.5-fold increase in NADPH levels ( $P < 0.01$ ) (Figure 6M) when compared to chow mice. NR therapy mice used NADPH to maintain the GSH redox state (Figure 6N). NADPH is an essential cofactor of glutathione reductase (GR), a key enzyme for catalyzing the recycling of reduced and oxidized glutathione (GSH and GSSG, respectively), and the production of GSH relies on the bioavailability of NADPH. To our knowledge, this is the first report of NR supplementation increasing NADPH and GSH levels in HFpEF hearts, both of which are essential for maintaining cellular redox homeostasis.

## DISCUSSION

Although recent preclinical data demonstrated rescue of HFpEF by replenishing NAD<sup>+</sup> using precursors such as NR<sup>8</sup> or NAM,<sup>7</sup> skepticism remains about the feasibility of this approach in human HFpEF because of myocardial NAMPT depletion. However, our data show that if adequate supply of NR can reach the heart, reduced NAMPT does not preclude NAD<sup>+</sup> repletion.

Despite our data suggesting that prophylactic supplementation of NR exerts favorable outcomes to

avert the onset of the HFpEF phenotype in mice, replication in human clinical trials is needed to validate these findings. In fact, in our murine model, therapeutic NR elevated NAMPT levels, facilitating its own replenishment of NAD<sup>+</sup>. The abundant increase in levels of NAM and its relationship to NAD<sup>+</sup> and other intermediates warrant further exploration with detailed fluxomic studies. Further, we did not explore potential recycling of NR into nicotinic acid by the gut microbiome, which could lead to the generation of NAD<sup>+</sup> via the Preiss-Handler pathway. Prophylactic supplementation of NR enacted a different program of salutary effects compared to NR treatment after the establishment of the phenotype. In both cases, NR was administered with ongoing HFD and L-NAME, with only the timing of NR commencement differing. Therapeutic NR administration was able to rescue the cardiac features of HFpEF and reverse HF in both male and female mice. However, it is important to note that there was a sex dependency of the prophylactic NR response, with the beneficial effects seen only in male mice. This could potentially be attributed to a sex-time interaction, given the shorter duration of the prophylactic protocol. Throughout the course of the prophylactic protocol, increases in weight and fat mass were only prevented in male mice and not female mice. Upon examining the potential underlying molecular changes in male prophylactic NR myocardium, we observed several unique molecular alterations. Among these changes, the increased expression of the antioxidant, cysteine-rich protein MT1 suggests a potential mitigation in inflammatory responses.<sup>40</sup> Prophylactic NR also resulted in changes in several proteins intrinsically linked to hypertrophic responses under increased workloads, including PRKG1 and PRKAA1.<sup>30,41</sup> The observed reduction in their expression levels might indicate a potential normalization effect brought on by NR administration. Other protein changes indicated prevention of fibrosis via UCHL1<sup>35</sup> and maintenance of lymphangiogenesis via LYVE1.<sup>42</sup> Although it was recently demonstrated that NAD<sup>+</sup> replenishment can rescue preclinical HFpEF,<sup>7,8</sup> the relative efficacy of this approach in comparison to mitigation of mediating risk factors via dietary intervention and weight loss has not been studied. Additionally, although both strategies seem plausible, the molecular mechanisms through which these therapeutic approaches mediate their effects remain unknown. To our knowledge, this is the first study to compare these strategies.

Although diet reversal could not fully restore cardiac function and rescue HFpEF, it led to a series of beneficial myocardial changes indicating metabolic improvements. Hearts from HFpEF mice showed a drastic metabolic shift from glucose to lipid use, which was attended by a host of deleterious changes, including up-regulation of proteins linked to the accumulation of toxic lipid species, fibrosis, diastolic dysfunction, and aberrant cardiac remodeling. Remarkably, diet reversal ameliorated all of these effects and restored myocardial insulin-dependent glucose uptake and glucose oxidation following the reversal of glucose intolerance and insulin resistance. The observed concomitant elevation in FASN and ACLY protein expressions, coupled with the decrease in PDK4 levels, underscores the heart's metabolic reprogramming in response to dietary shifts. Transitioning from an HFD to a chow diet elevates carbohydrate intake in the heart that, when not immediately used for energy, can be redirected into fatty acid synthesis through de novo lipogenesis. However, in spite of these benefits, diet reversal was unable to restore cardiac function fully, highlighting the shortcomings of dietary intervention in treating HFpEF.

In this study, we further explored the mechanistic pathways via which NR therapy did rescue cardiac function in HFpEF. Our findings resonate with the findings by Tong et al<sup>8</sup> and Abdellatif et al<sup>7</sup> demonstrating that the replenishment of NAD<sup>+</sup> enhances mitochondrial function and myocardial energetics. Notably, we observed that NR therapy was successful in both restoring the NADPH-mediated regeneration of reduced glutathione from its oxidized form and in boosting energetic flux. Several clinical studies have reported that the production of reactive oxygen species (ROS) is increased in HFpEF myocardium.<sup>43-45</sup> An excess generation of ROS levels beyond antioxidant capacity leads to oxidative stress that damages the myocardium. Our findings suggest that NR therapy enacts a defense response against myocardial oxidants by increasing production of mitochondrial NADPH, an essential source of reducing power for the glutathione antioxidant system, ultimately driving glutathione reduction and, therefore, preventing ROS-induced cardiomyocyte injury.

Further, our data indicate that NR therapy overcomes 2 critical impasses imposed on the glycolytic pathway, plausibly through up-regulation of LDHB to divert lactate back into pyruvate for generation of

acetyl-CoA and via branched-chain amino acid oxidation as an alternative source of acetyl-CoA for the TCA cycle. Together, these alterations facilitated an increase in TCA flux for oxidative phosphorylation, thereby increasing ATP production in the hearts of HFpEF mice.

**STUDY LIMITATIONS.** Although our study primarily focused on NAD<sup>+</sup> and NAD<sup>+</sup>-dependent enzymes such as SIRT3, investigating other deacetylation processes, such as the impact of SIRT1 on PGC1 $\alpha$  (which plays a significant role in mitochondrial biogenesis and function), is warranted but extends beyond the scope of this current paper. Although LC-MS/MS is now a widely accepted method known for its high sensitivity, specificity, resolution, fidelity, accuracy, and precision, we did not independently validate the protein changes reported in the figures (Supplemental Table 2) using another methodology. Although our human samples displayed diastolic impairment, they were not from patients with the full spectrum of HFpEF. Obtaining LV myocardium from HFpEF patients presents a significant challenge and as is typically feasible only when another medical indication, such as a surgical valve repair, is required, although structural heart diseases such as this alter the phenotype. Conceivably, patients with aortic stenosis (resulting in a pressure-loaded ventricle) and concomitant metabolic stress, such as coexisting obesity and type 2 diabetes mellitus, would be more representative of a large subset of HFpEF patients. The opportunity to retrieve endomyocardial biopsy specimens during aortic valve replacement procedures is crucial. Conducting studies using these biopsy specimens is absolutely critical for advancing our understanding of mechanistic insight into the pathogenesis of HFpEF.

## CONCLUSIONS

In this study, we report several novel findings that are instructive for therapeutic approaches to cardiac diastolic impairment and HFpEF. Critically, we showed that, in human myocardium with diastolic dysfunction, NAMPT depletion does not preclude replenishment of NAD<sup>+</sup> with the stable precursor NR. In the murine model, dietary intervention enacted a wide range of beneficial myocardial molecular changes; however, these were insufficient to rescue

HFpEF in either male or females. Prophylactic NR could avert obesity in male HFpEF, but therapeutic NR treatment after the establishment of the HFpEF phenotype could not in males or females. Nevertheless, therapeutic NR fully rescued diastolic impairment and HF in both males and females, inducing synergistic antioxidant protection and enhanced energetics in the myocardium. Indeed, prophylactic and therapeutic NR resulted in distinct molecular benefits, suggesting important considerations for translation to the clinic. The findings obtained from this investigation lay the groundwork for more comprehensive mechanistic studies using genetic manipulation.

**ACKNOWLEDGMENTS** The authors thank SydneyMS for providing the instrumentation used in this study. The authors thank the patients and staff of St Vincent's Hospital Sydney and Royal Prince Alfred Hospital. The authors acknowledge Prof Cris dos Remedios and the late Dr Victor Chang, AO, who established the Sydney Heart Bank in 1989. The authors thank Prof Roland Stoker for providing the high-resolution respirometry for this study and Dr Stephanie Kong from Heart Research Institute for her guidance and training on the Oroboros oxygraph. The authors thank the Baird Institute for their support with biobanking.

## FUNDING SUPPORT AND AUTHOR DISCLOSURES

This work was supported by the Sydney Medical School Foundation (Dr O'Sullivan); Sydney Cardiovascular Fellowship (Dr O'Sullivan), NSW Health Early-Mid Career Fellowship and Clinician-Scientist Awards (Dr O'Sullivan; DOH1003 and DOH1006), National Heart Foundation Future Leader Fellowship (Dr O'Sullivan; NHF104853), National Heart Foundation Future Leader Fellowship (Dr Koay; NHF107180), NSW Cardiovascular Collaborative Grant (Dr Koay), and philanthropic support from The University of Sydney donors (Dr Lal). All other authors have reported that they have no relationships relevant to the contents of this paper to disclose.

**ADDRESSES FOR CORRESPONDENCE:** Dr Yen Chin Koay, Faculty of Medicine and Health, School of Medical Sciences, University of Sydney, Eastern Avenue, Sydney, NSW 2050, Australia. E-mail: [yen.koay@sydney.edu.au](mailto:yen.koay@sydney.edu.au). OR Prof John F. O'Sullivan, Faculty of Medicine and Health, School of Medical Sciences, University of Sydney, Eastern Avenue, Sydney, NSW 2050, Australia. E-mail: [john.osullivan@sydney.edu.au](mailto:john.osullivan@sydney.edu.au).

## PERSPECTIVES

**COMPETENCY IN MEDICAL KNOWLEDGE:** HFpEF is a type of HF that is often associated with LV diastolic dysfunction and risk factors like hypertension, obesity, and metabolic diseases. In our study, we investigate the effectiveness of NAD<sup>+</sup> repletion in an HFpEF mouse model, directly comparing it to conventional approaches such as dietary intervention and weight loss. The results from our research underscore the significance of the early identification and intervention in HFpEF management, aligning with the latest American College of Cardiology/American Heart Association/Heart Failure Society of America guidelines. This knowledge can assist clinicians in recognizing and effectively managing “at-risk” HF patients at stages A and B.

**TRANSLATIONAL OUTLOOK:** The research on NAD<sup>+</sup> in HF marks a significant step in translational medicine, suggesting new directions for clinical trials and personalized medicine approaches. Our study suggests that NAD<sup>+</sup> repletion, both prophylactic and therapeutic, may offer a viable and promising approach in clinical settings, despite previous concerns about the feasibility because of NAMPT depletion. While acknowledging the benefits of dietary intervention, our research suggests that these measures alone may not suffice in reversing HFpEF. The comparison of different NAD<sup>+</sup> repletion strategies provides a basis for future clinical trials and research, aiming to refine these approaches for human application.

## REFERENCES

1. Tam MC, Lee R, Cascino TM, Konerman MC, Hummel SL. Current perspectives on systemic hypertension in heart failure with preserved ejection fraction. *Curr Hypertens Rep.* 2017;19:1-11.
2. Savji N, Meijers WC, Bartz TM, et al. The association of obesity and cardiometabolic traits with incident HFpEF and HFrEF. *J Am Coll Cardiol HF.* 2018;6:701-709.
3. Schiattarella GG, Altamirano F, Tong D, et al. Nitrosative stress drives heart failure with preserved ejection fraction. *Nature.* 2019;568:351-356.
4. Kitzman DW, Brubaker P, Morgan T, et al. Effect of caloric restriction or aerobic exercise training on peak oxygen consumption and quality of life in obese older patients with heart failure with preserved ejection fraction: a randomized clinical trial. *JAMA.* 2016;315:36-46.
5. Wang Z, Ying Z, Bosy-Westphal A, et al. Specific metabolic rates of major organs and tissues across adulthood: evaluation by mechanistic model of resting energy expenditure. *Am J Clin Nutr.* 2010;92:1369-1377.
6. Tannous C, Booz GW, Altara R, et al. Nicotinamide adenine dinucleotide: biosynthesis, consumption and therapeutic role in cardiac diseases. *Acta Physiol.* 2021;231:e13551.
7. Abdellatif M, Trummer-Herbst V, Koser F, et al. Nicotinamide for the treatment of heart failure with preserved ejection fraction. *Sci Transl Med.* 2021;13:eabd7064.
8. Tong D, Schiattarella GG, Jiang N, et al. NAD<sup>+</sup> repletion reverses heart failure with preserved ejection fraction. *Circ Res.* 2021;128:1629-1641.
9. Heidenreich PA, Bozkurt B, Aguilar D, et al. 2022 AHA/ACC/HFSA guideline for the management of heart failure: a report of the American College of Cardiology/American Heart Association Joint Committee on Clinical Practice Guidelines. *J Am Coll Cardiol.* 2022;79(17):e263-e421.
10. Mollova M, Bersell K, Walsh S, et al. Cardiomyocyte proliferation contributes to heart growth in young humans. *Proc Natl Acad Sci U S A.* 2013;110:1446-1451.
11. Lal S, Li A, Allen D, et al. Best practice bio-banking of human heart tissue. *Biophys Rev.* 2015;7:399-406.
12. Polizzotti BD, Ganapathy B, Walsh S, et al. Neuregulin stimulation of cardiomyocyte regeneration in mice and human myocardium reveals a therapeutic window. *Sci Transl Med.* 2015;7:281ra245.
13. Sequeira V, Najafi A, Wijnker PJM, et al. ADP-stimulated contraction: a predictor of thin-filament activation in cardiac disease. *Proc Natl Acad Sci U S A.* 2015;112:E7003-E7012.
14. Lange S, Gehmlich K, Lun AS, et al. MLP and CARP are linked to chronic PKC $\alpha$  signalling in dilated cardiomyopathy. *Nat Commun.* 2016;7:1-11.
15. Crossman DJ, Shen X, Jüllig M, et al. Increased collagen within the transverse tubules in human heart failure. *Cardiovasc Res.* 2017;113:879-891.
16. Mamidi R, Li J, Gresham KS, et al. Dose-dependent effects of the myosin activator ome-camtiv mecarbil on cross-bridge behavior and force generation in failing human myocardium. *Circ Heart Fail.* 2017;10:e004257.
17. Cao J, Koay YC, Quek L-E, Parker B, Lal S, O'Sullivan JF. Myocardial substrate changes in advanced ischaemic and advanced dilated human heart failure. *Eur J Heart Fail.* 2019;21:1042-1045.
18. van Heesch S, Witte F, Schneider-Lunitz V, et al. The translational landscape of the human heart. *Cell.* 2019;178:242-260.e229.
19. Li M, Parker BL, Pearson E, et al. Core functional nodes and sex-specific pathways in human ischaemic and dilated cardiomyopathy. *Nat Commun.* 2020;11:1-12.
20. Lal S, Nguyen L, Tezone R, et al. Tissue microarray profiling in human heart failure. *Proteomics.* 2016;16:2319-2326.
21. Schnelle M, Catibog N, Zhang M, et al. Echocardiographic evaluation of diastolic function in mouse models of heart disease. *J Mol Cell Cardiol.* 2018;114:20-28.
22. Koay YC, Wali JA, Luk AWS, et al. Ingestion of resistant starch by mice markedly increases microbiome-derived metabolites. *FASEB J.* 2019;33:8033-8042.
23. Koay YC, Stanton K, Kienzle V, et al. Effect of chronic exercise in healthy young male adults: a metabolomic analysis. *Cardiovasc Res.* 2020;117:613-622.
24. Trammell SA, Brenner C. Targeted, LCMS-based metabolomics for quantitative measurement of NAD<sup>+</sup> metabolites. *Comput Struct Biotechnol J.* 2013;4:e201301012.
25. Harney DJ, Hutchison AT, Hatchwell L, et al. Proteomic analysis of human plasma during intermittent fasting. *J Proteome Res.* 2019;18:2228-2240.
26. Martinez-Huenchullan SF, Shipsey I, Hatchwell L, Min D, Twigg SM, Larance M. Blockade of high-fat diet proteomic phenotypes using exercise as prevention or treatment. *Mol Cell Proteomics.* 2021;20:100027.
27. Demichev V, Messner CB, Vernardis SI, Lilley KS, Ralser M. DIA-NN: neural networks and interference correction enable deep proteome coverage in high throughput. *Nat Methods.* 2020;17:41-44.

28. Fusco-Allison G, Li DK, Hunter B, et al. Optimizing the discovery and assessment of therapeutic targets in heart failure with preserved ejection fraction. *ESC Heart Failure*. 2021;8:3643-3655.
29. Naing P, Forrester D, Kangaharan N, Muthumala A, Myint SM, Playford D. Heart failure with preserved ejection fraction: 'a growing global epidemic.'. *Aust J Gen Pract*. 2019;48:465-471.
30. Schwaerzer GK, Casteel DE, Cividini F, et al. Constitutive protein kinase G activation exacerbates stress-induced cardiomyopathy. *Br J Pharmacol*. 2022;179(11):2413-2429.
31. Duerr GD, Dewald D, Schmitz EJ, et al. Metallothioneins 1 and 2 modulate inflammation and support remodeling in ischemic cardiomyopathy in mice. *Mediators Inflamm*. 2016;2016:7174127.
32. Hofsteen P, Robitaille AM, Strash N, et al. ALPK2 promotes cardiogenesis in zebrafish and human pluripotent stem cells. *IScience*. 2018;2:88-100.
33. Pang T, Su X, Wakabayashi S, Shigekawa M. Calcineurin homologous protein as an essential cofactor for Na<sup>+</sup>/H<sup>+</sup> exchangers. *J Biol Chem*. 2001;276:17367-17372.
34. Lei Q, Yi T, Li H, et al. Ubiquitin C-terminal hydrolase L1 (UCHL1) regulates post-myocardial infarction cardiac fibrosis through glucose-regulated protein of 78 kDa (GRP78). *Sci Rep*. 2020;10:1-12.
35. Bi H-L, Zhang X-L, Zhang Y-L, et al. The deubiquitinase UCHL1 regulates cardiac hypertrophy by stabilizing epidermal growth factor receptor. *Sci Adv*. 2020;6:eaax4826.
36. Bizou M, Itier R, Majdoubi M, et al. Cardiac macrophage subsets differentially regulate lymphatic network remodeling during pressure overload. *Sci Rep*. 2021;11:1-19.
37. Gil-Cayuela C, Roselló-Lletí E, Ortega A, et al. New altered non-fibrillar collagens in human dilated cardiomyopathy: role in the remodeling process. *PLoS One*. 2016;11:e0168130.
38. Zuccolotto-dos-Reis FH, Escarso SHA, Araujo JS, Espreafico EM, Alberici LC, Sobreira CFD. Acetyl-CoA-driven respiration in frozen muscle contributes to the diagnosis of mitochondrial disease. *Eur J Clin Invest*. 2021;51:e13574.
39. Xiao W, Wang R-S, Handy DE, Loscalzo J. NAD (H) and NADP (H) redox couples and cellular energy metabolism. *Antioxid Redox Signal*. 2018;28:251-272.
40. Inoue K, Takano H, Shimada A, Satoh M. Metallothionein as an anti-inflammatory mediator. *Mediators Inflamm*. 2009;2009:101659.
41. Gupta R, Singh-Gupta V, Hani N. Abstract 259: dysregulation of AMP-activated protein kinase-alpha isoforms in left ventricular myocardium of dogs with chronic heart failure. *Circ Res*. 2020;127. [https://www.ahajournals.org/doi/10.1161/res.127.suppl\\_1.259](https://www.ahajournals.org/doi/10.1161/res.127.suppl_1.259)
42. Karunamuni G. *The Cardiac Lymphatic System*. Springer; 2013.
43. Vitiello D, Harel F, Touyz RM, et al. Changes in cardiopulmonary reserve and peripheral arterial function concomitantly with subclinical inflammation and oxidative stress in patients with heart failure with preserved ejection fraction. *Int J Vasc Med*. 2014;2014:917271.
44. Negi SI, Jeong E-M, Shukrullah I, et al. Renin-angiotensin activation and oxidative stress in early heart failure with preserved ejection fraction. *Biomed Res Int*. 2015;2015:825027.
45. Zuo L, Chuang C-C, Hemmelgarn BT, Best TM. Heart failure with preserved ejection fraction: defining the function of ROS and NO. *J Appl Physiol*. 2015;119:944-951.

---

**KEY WORDS** diastolic heart failure, heart failure, NAD<sup>+</sup> repletion

---

**APPENDIX** For supplemental Methods, tables, figures, and references, please see the online version of this paper.